

PDF hosted at the Radboud Repository of the Radboud University Nijmegen

The following full text is a publisher's version.

For additional information about this publication click this link.

<http://hdl.handle.net/2066/29740>

Please be advised that this information was generated on 2021-06-15 and may be subject to change.

Relativistic oscillator of constant period

Jung-Hoon Kim,¹ Seung-Woo Lee,¹ Hans Maassen,² and Hai-Woong Lee¹

¹*Department of Physics, Korea Advanced Institute of Science and Technology, Taejon 305-701, Korea*

²*Department of Mathematics, Catholic University of Nijmegen, Toernooiveld 1, 6525 ED Nijmegen, The Netherlands*

(Received 15 November 1995)

A relativistic oscillator whose period is independent of its energy is of great fundamental importance in both relativistic classical mechanics and relativistic quantum mechanics. In this work theoretical and computational investigations of such a constant period oscillator are reported, with emphasis on basic mathematical and physical properties of the oscillator.

PACS number(s): 03.30.+p, 03.65.-w

I. INTRODUCTION

The simple harmonic oscillator (SHO) is undoubtedly of great importance in both classical mechanics and quantum mechanics. It represents the most fundamental system for which the equation of motion, whether it is classical Hamilton's equations or quantum-mechanical Schrödinger equation, can be handled in a simple analytic way. Classically, the unique simplicity of the SHO stems from the fact that the period of oscillation is independent of the oscillator energy. This unique property manifests itself in the quantum world as equally spaced energy levels.

It should be noted, however, that the SHO no longer occupies such a unique place once one enters the relativistic regime. The period of oscillation is no longer independent of energy if the oscillator moves at relativistic velocities [1]. It can then be immediately suggested that in the relativistic regime the system that plays a fundamental role as the SHO is an oscillator whose period is independent of energy in the entire energy range, both nonrelativistic and relativistic. Such an oscillator, which we refer to as the constant period oscillator (CPO), is the subject of this work.

Despite the fundamental importance of the CPO in relativistic classical and quantum mechanics, there appears to be very little work on the subject of the CPO in the past. This may be due partly to the fact that the potential that governs the motion of the CPO, which we refer to as the constant period potential (CPP), cannot be expressed in a simple analytic form. It is obvious that the CPP should behave like a harmonic potential in the nonrelativistic limit [$V(q) \ll mc^2$] and like a square-well potential in the ultrarelativistic limit [$V(q) \gg mc^2$]. Thus the curve representing the CPP should increase as q^2 near $q=0$ but should become continuously steeper at larger q until it becomes practically a vertical line.

The problem of determining the shape of potential that yields a constant period falls into the category of the "inverse problem." In the inverse scattering problem, for example, the intermolecular potential is sought from given scattering data [2,3]. Our problem, a special case of the inverse problem in which the potential is determined from a given energy dependence of the period $T=T(E)$, is similar in mathematical structure to the well-known "tautochrone" problem [4]. As our main interest lies in the relativistic motion, it has much in common in particular with the relativistic tautochrone problem [5]. To our knowledge the first attempt

to determine the shape of the CPP in the relativistic region was reported by Funke and Ratis [6]. They used the technique of Laplace transform, a standard technique used in the tautochrone problem [4], and obtained a general expression relating $T(E)$ and the corresponding potential. Based on this expression, they obtained a power series expression for the CPP.

In this work we investigate fundamental mathematical and physical properties of the CPO. Since no simple analytic treatment can be given to the CPO, we first obtained the curve representing the CPP via numerical computation. This provides the "exact" potential against which theories of and approximations on the CPO can be tested. Analytic treatments based on the technique of Laplace transform are, however, still valuable because some fundamental mathematical properties such as scaling properties and approximate behavior in the nonrelativistic and ultrarelativistic limits can be found from them. Based upon these mathematical properties, we were able to introduce approximate formulas that accurately reproduce the CPP. Using the approximate formulas as well as the exact numerical potential, we then computed the classical time evolution and the quantum energy eigenvalues of the CPO.

We hope that the analysis presented here provides the basic knowledge that should help to enhance our understanding of relativistic classical mechanics and relativistic quantum mechanics. The direct motivation for this study came from our previous study of the "relativistic chaos" [7,8], chaos exhibited by a system undergoing relativistic motion. We have found that even a simple harmonic oscillator that is free of chaos in the nonrelativistic regime can exhibit chaos if it is driven to relativistic velocities [7]. This is essentially because the period of the SHO becomes energy dependent at relativistic energies. In general, the way the period depends on energy takes a different form and consequently some interesting new phenomena such as an appearance of new nonlinear resonances leading to chaos [8] and zero dispersion nonlinear phenomena [9,10] can occur, as one moves from the nonrelativistic region to the relativistic region. In any case, at least according to the first-order resonance theory [11], in order for nonlinear resonances to be formed and chaos to be exhibited by an oscillator driven by an external force, the period of oscillation should vary with respect to energy [7,8]. Thus the system that is completely free of chaos, at least in the first-order theory, in both nonrelativistic

and relativistic regions must be an oscillator whose period is independent of energy in the entire energy range. Such a system is obviously the CPO that we investigate in this work.

II. THEORETICAL ANALYSIS OF THE CONSTANT PERIOD POTENTIAL

Let $V(q)$, assumed to be symmetric about $q=0$, be the constant period potential that we seek. The energy of a particle of mass m oscillating under the influence of the potential $V(q)$ is

$$E = \sqrt{p^2 c^2 + m^2 c^4} - mc^2 + V(q), \quad (1)$$

where p is the momentum and c the speed of light. The action variable I is given by

$$\begin{aligned} I = I(E) &= \frac{1}{2\pi} \oint p dq \\ &= \frac{2}{\pi c} \int_0^b \sqrt{[E + mc^2 - V(q)]^2 - m^2 c^4} dq, \end{aligned} \quad (2)$$

where $b = V^{-1}(E)$ represents the amplitude of oscillation. Alternatively, the action variable can be written as

$$\begin{aligned} I(E) &= \frac{1}{2\pi} \oint q dp = \frac{4}{2\pi} \int_0^{P_{\max}} V^{-1}(E + mc^2 \\ &\quad - \sqrt{p^2 c^2 + m^2 c^4}) dp, \end{aligned} \quad (3)$$

where P_{\max} is the maximum momentum

$$P_{\max} = \frac{1}{c} \sqrt{(E + mc^2)^2 - m^2 c^4}. \quad (4)$$

Letting

$$\kappa = \sqrt{p^2 c^2 + m^2 c^4} - mc^2, \quad (5)$$

we can rewrite Eq. (3) as

$$I(E) = \frac{2}{\pi c} \int_0^E V^{-1}(E - \kappa) \frac{\kappa + mc^2}{\sqrt{\kappa(\kappa + 2mc^2)}} d\kappa. \quad (6)$$

Let us recall that at a given energy E the action variable $I(E)$ and the period $T(E)$ of oscillation are related by $\partial I(E)/\partial E = T(E)/2\pi$. For our constant period oscillator, $T(E)$ is just a constant, which we denote simply by T . Thus we have, for the case of the CPO,

$$I(E) = \frac{T}{2\pi} E. \quad (7)$$

Equations (6) and (7) yield

$$\int_0^E V^{-1}(E - \kappa) \frac{\kappa + mc^2}{\sqrt{\kappa(\kappa + 2mc^2)}} d\kappa = \frac{cT}{4} E. \quad (8)$$

Equation (8) is of convolution type to which the technique of Laplace transform is often applied with success. We thus take the Laplace transform of both sides of Eq. (8) and obtain

$$f(\lambda)g(\lambda) = \frac{cT}{4} \frac{1}{\lambda^2}, \quad (9)$$

where

$$f(\lambda) = L\{V^{-1}(E)\} = \int_0^\infty e^{-\lambda E} V^{-1}(E) dE \quad (10)$$

and

$$g(\lambda) = L\left\{ \frac{E + mc^2}{\sqrt{E(E + 2mc^2)}} \right\} = \int_0^\infty e^{-\lambda E} \frac{E + mc^2}{\sqrt{E(E + 2mc^2)}} dE. \quad (11)$$

The function $g(\lambda)$ can immediately be evaluated to yield

$$g(\lambda) = mc^2 e^{\lambda mc^2} K_1(\lambda mc^2), \quad (12)$$

where K_1 denotes the modified Bessel function of order one. Substituting Eq. (12) into Eq. (9), we have

$$f(\lambda) = \int_0^\infty e^{-\lambda E} V^{-1}(E) dE = \frac{cT}{4mc^2} \frac{1}{\lambda^2 e^{\lambda mc^2} K_1(\lambda mc^2)}. \quad (13)$$

This is the formula obtained by Funke and Ratis [6]. In principle one can determine $V(q)$ from Eq. (13) as follows. One first determines $f(\lambda)$ from Eq. (13). Taking the inverse Laplace transform of $f(\lambda)$, one then obtains V^{-1} . The knowledge of V^{-1} should allow determination of V . In practice, however, difficulty arises because the inverse Laplace transform of $f(\lambda)$ is extremely hard to evaluate and thus one often needs to rely on direct numerical computation. Before closing the section we rewrite Eq. (13) in a slightly more convenient form

$$\int_0^\infty e^{-yt} \left[\frac{4}{cT} V^{-1}(tmc^2) \right] dt = \frac{1}{y^2 e^y K_1(y)}. \quad (14)$$

III. MATHEMATICAL PROPERTIES OF THE CONSTANT PERIOD POTENTIAL

In this section we first present the constant period potential evaluated numerically using a computer. We then present a theoretical analysis of the fundamental mathematical properties of the CPP.

A. Numerical evaluation of the constant period potential

In order to obtain the actual shape of the CPP, it is much easier and more straightforward to employ direct numerical computation than to use Eq. (13) or (14). Basically, one starts with $V(q_0=0)=0$ and determines $V(q_1=\Delta q)$ by assuming that the curve is harmonic, $V(q_1) = \frac{1}{2}m(2\pi q_1/T)^2$. With $V(q_1)$ and $V(q_0)$ known, we then determine the next point $V(q_2=2\Delta q)$ by assuming that the three points $V(q_0)$, $V(q_1)$, and $V(q_2)$ lie on a parabola and finding the

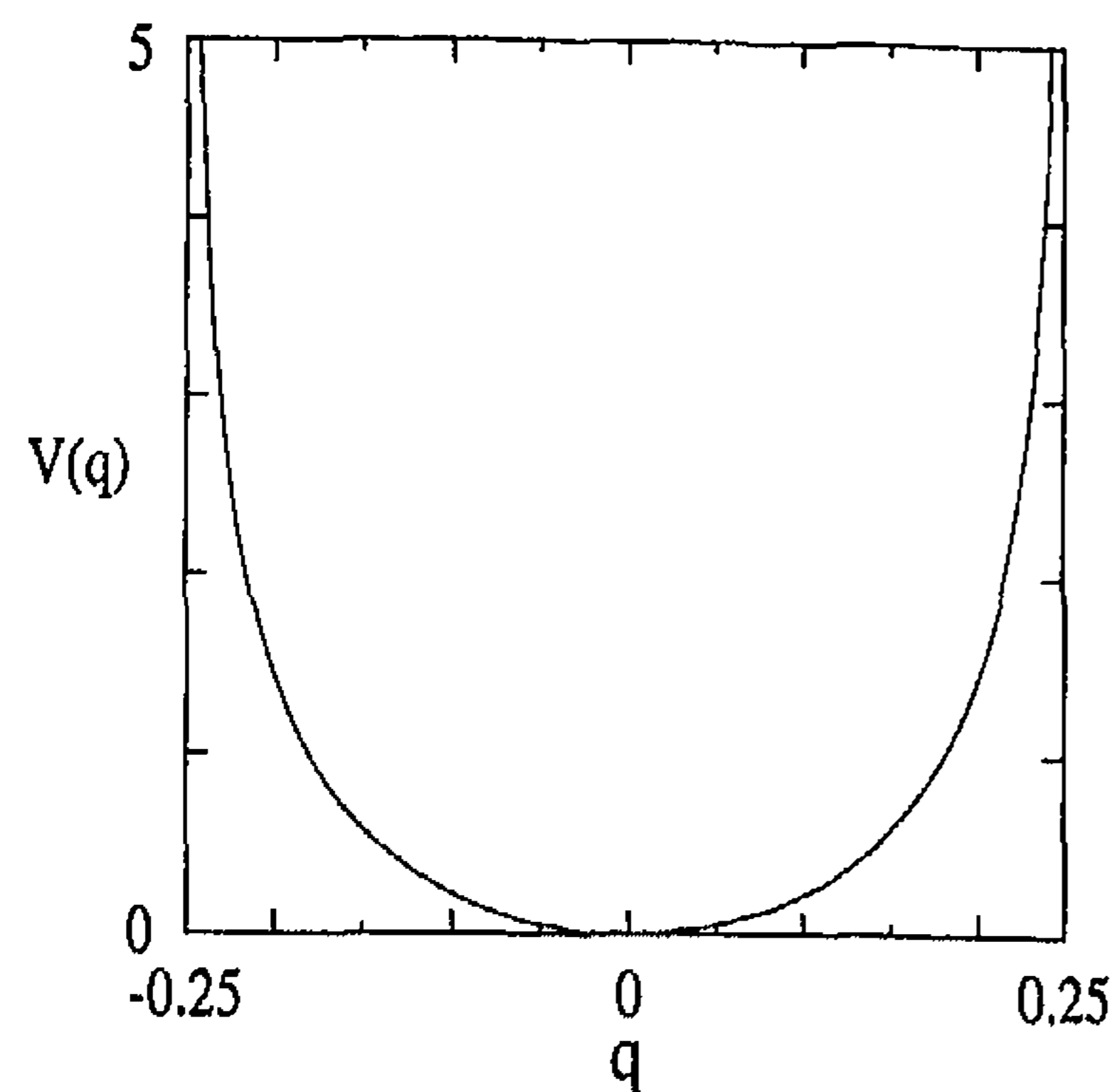


FIG. 1. Constant period potential. $m=T=c=1$.

parabola that best yields the desired period T for the motion with amplitude $b=q_2$. Proceeding the same way, $V(q_n = n\Delta q)$ can be determined from the previously determined points $V(q_{n-1})$ and $V(q_{n-2})$ by the method of parabolic fitting. In our computation of the CPP for the case $m=T=c=1$, we divided the interval between $q=0$ and $q=cT/4=0.25$ into 10 000 equal segments, i.e., Δq was taken to be 2.5×10^{-5} . The computation of period was carried out using the Runge-Kutta method with a time step of $1/20\,000$. At each interval, the correct point $V(q_n)$ was sought until the computed period yields the correct value of 1 within an error of 10^{-5} .

In Fig. 1 we present the CPP we obtained via direct numerical computation for the case $m=T=c=1$. In the vicinity of $q=0$ the curve is harmonic, i.e.,

$$V(q) \sim \frac{1}{2}m \left(\frac{2\pi q}{T} \right)^2 = 2\pi^2 q^2 \text{ as } q \rightarrow 0, \quad (15)$$

whereas it is almost a vertical line as q approaches $\pm cT/4 = \pm \frac{1}{4}$, i.e.,

$$V(q) \rightarrow \infty \text{ as } q \rightarrow \pm \frac{cT}{4} = \pm \frac{1}{4}. \quad (16)$$

B. Scaling properties

The scaling properties of the CPP can best be analyzed with Eq. (14). Since the right-hand side of Eq. (14) is a function only of y , we conclude that the quantity in the square brackets on the left-hand side must be a function only of t , i.e.,

$$\frac{4}{cT} V^{-1}(tmc^2) = L^{-1} \left\{ \frac{1}{y^2 e^y K_1(y)} \right\} \equiv F(t). \quad (17)$$

Equation (17) can be expressed as

$$V \left(\frac{cT}{4} F(t) \right) = mc^2 t \quad (18)$$

or, setting $q = (cT/4) F(t)$, as

$$V(q) = mc^2 F^{-1} \left(\frac{4q}{cT} \right). \quad (19)$$

Equation (19) indicates that V scales linearly with mass m and depends not on q and T separately but on q/T . Thus, if $V(q)$ represents the potential that yields a period T for a particle of mass m , the potential that yields the same period T for a particle of mass $2m$ is $2V(q)$, while the potential that yields a period $2T$ for a particle of the same mass m is $V(q/2)$. In other words, let $V(q)$ be the potential that yields a period of 1 for an oscillator of mass 1. Then the potential that yields a period of T for an oscillator of mass m must be given by $mV(q/T)$. We note that the above scaling properties of the CPP are shared by the simple harmonic potential $V(q) = \frac{1}{2}m(2\pi q/T)^2$.

C. Nonrelativistic limit

The behavior of the CPP in the vicinity of $q=0$ [or in the nonrelativistic region in which $V(q) \ll mc^2$] can be determined by noting that the modified Bessel function K_1 can be expanded as

$$K_1(z) = \sqrt{\frac{\pi}{2z}} e^{-z} \left[1 + \frac{3}{8z} - \frac{15}{2(8z)^2} + \frac{105}{2(8z)^3} - \dots \right]. \quad (20)$$

Using Eq. (20) to expand the right-hand side of Eq. (13) in series of $1/z = 1/\lambda mc^2$ and evaluating the inverse Laplace transform of each term in the series separately, we obtain a series solution for the CPP, which reads

$$V(q) = \frac{1}{2}m \left(\frac{2\pi q}{T} \right)^2 \left[1 + \frac{1}{4} \left(\frac{2\pi q}{cT} \right)^2 + \frac{3}{40} \left(\frac{2\pi q}{cT} \right)^4 + \frac{11}{448} \left(\frac{2\pi q}{cT} \right)^6 + \dots \right]. \quad (21)$$

As expected, the leading term in Eq. (21) coincides with the harmonic potential of the same period.

D. Ultrarelativistic limit

When the oscillator moves with ultrarelativistic energy ($E \gg mc^2$), its motion near the turning points is governed by the potential near $q = \pm cT/4$. The approximate behavior of the CPP in the vicinity of $q = cT/4$ [or in the ultrarelativistic region in which $V(q) \gg mc^2$] can be found by utilizing the power series of the modified Bessel function

$$K_1(z) = \frac{1}{z} \left[1 + \frac{z^2}{2} \left(\ln \frac{z}{2} - \gamma - \frac{1}{2} \right) + \frac{z^4}{16} \left(\ln \frac{z}{2} - \gamma - \frac{5}{4} \right) + \dots \right], \quad (22)$$

where γ is the Euler constant $\gamma \cong 0.577$. Substituting Eq. (22) into Eq. (14) and evaluating the inverse Laplace transform term by term, one obtains after lengthy but straightforward algebra

$$V(q) = mc^2 + \frac{mc^2}{\sqrt{2}} \frac{1}{\sqrt{1 - \frac{4q}{cT}}} \left[1 + 6 \left(1 - \frac{4q}{cT} \right) \right. \\ \left. \times \ln \frac{1}{\sqrt{2} \sqrt{1 - \frac{4q}{cT}}} - \frac{1}{8} (58 - 48 \ln 2) \left(1 - \frac{4q}{cT} \right) + \dots \right]. \quad (23)$$

In the immediate vicinity of $q = cT/4$, it often is sufficient to keep only the leading term in Eq. (23) and take

$$V(q) \cong mc^2 + \frac{mc^2}{\sqrt{2}} \frac{1}{\sqrt{1 - \frac{4q}{cT}}}. \quad (24)$$

E. Approximate formulas

Since no simple analytic formula exists for the CPP, it will be useful if one finds an approximate formula that closely reproduce the exact CPP for the entire range of q , $-cT/4 < q < cT/4$. It of course is desirable that the approximate formula be consistent with the scaling properties represented by Eq. (19) and the limiting forms indicated by Eqs. (21) and (23).

Among several formulas we tested, we found the following two to accurately represent the CPP:

$$V_1(q) = \frac{mc^2 \pi^2}{8N} \left\{ \frac{1}{\left[1 - \left(\frac{4q}{cT} \right)^2 \right]^N} - 1 \right\} \quad (25)$$

and

$$V_2(q) = \frac{mc^2}{\alpha} \left\{ \frac{\cosh \left[\beta \left(\frac{2\pi q}{cT} \right)^2 \right]}{\cos^\alpha \left(\frac{2\pi q}{cT} \right)} - 1 \right\}. \quad (26)$$

In Eq. (26), α and β are constants $\alpha = 0.3$ and $\beta = 0.05$. In Eq. (25) the constant N can be chosen to fit the exact CPP best. Our numerical analysis showed that the choice $N = 0.24$ yields the best fit. With $N = 0.24$ Eq. (25) was found to yield a constant period within 0.13%. The choice $N = 0.25$ is also very good with a fractional error in period within 0.2%. Equation (26) works even better and yields a constant period within 0.08%.

Both formulas (25) and (26) satisfy the scaling condition Eq. (19) and yield the correct leading term $\frac{1}{2}m(2\pi q/T)^2$ at small q . The main source of error in Eqs. (25) and (26) lies in their behavior near $q = \pm cT/4$. Although they diverge as $q = \pm cT/4$ is approached, neither of the two formulas is quite consistent with Eq. (24). Nevertheless, as far as the

TABLE I. Exact constant period potential $V(q)$ and the approximate potentials $V_1(q)$ with $N = 0.25$ and $V_2(q)$. $m = T = c = 1$.

q	$V(q)$	$V_1(q)$	$V_2(q)$
0	0	0	0
0.025	0.0124	0.0124	0.0124
0.050	0.0506	0.0506	0.0506
0.075	0.1176	0.1177	0.1176
0.100	0.2195	0.2199	0.2195
0.125	0.3671	0.3680	0.3670
0.150	0.5801	0.5825	0.5800
0.175	0.8990	0.9047	0.8988
0.200	1.422	1.436	1.423
0.225	2.503	2.540	2.511

period of oscillation is concerned, the detailed shape of the potential near $q = \pm cT/4$ does not matter much as long as the potential diverges sufficiently fast when $q = \pm cT/4$ is approached. Thus the dynamics of the CPO can be described with high accuracy even if computation is performed using the approximate potential $V_1(q)$ or $V_2(q)$.

In Table I we tabulate values of $V_1(q)$ (with $N = 0.25$) and $V_2(q)$ at some representative points and compare with the exact numerical values obtained by direct computation as described in Sec. III A for the case $m = T = c = 1$. It is seen that both $V_1(q)$ and $V_2(q)$ agree well with the exact CPP, except near $q = \pm cT/4 = \pm 0.25$. A more detailed comparison in the region near $q = cT/4 = 0.25$ is given in Table II, where the exact numerical potential $V(q)$, the approximate potentials $V_1(q)$ and $V_2(q)$, and the approximate formulas Eqs. (23) and (24) are computed for $0.248 \leq q < 0.25$. As expected Eqs. (23) and (24) give a better fit to the exact potential than $V_1(q)$ or $V_2(q)$ in the region near $q = \pm cT/4$.

IV. PHYSICAL PROPERTIES OF THE CONSTANT PERIOD OSCILLATOR

In this section fundamental physical properties of both the classical CPO and the quantum-mechanical CPO are investigated. Our computations have been performed using the approximate potential $V_2(q)$ as well as the exact numerical potential. In all cases, the approximate potential $V_2(q)$ and the exact potential produced essentially the identical results.

TABLE II. Exact constant period potential $V(q)$, the approximate potentials $V_1(q)$ with $N = 0.25$ and $V_2(q)$, and the approximate formulas Eqs. (23) and (24). $m = T = c = 1$.

q	$V(q)$	$V_1(q)$	$V_2(q)$	Eq. (23)	Eq. (24)
0.24800	9.265	8.954	9.149	9.495	8.906
0.24825	9.830	9.424	9.660	10.03	9.452
0.24850	10.52	9.986	10.28	10.69	10.13
0.24875	11.41	10.68	11.04	11.54	11.00
0.24900	12.60	11.57	12.04	12.69	12.18
0.24925	14.33	12.80	13.42	14.38	13.91
0.24950	17.21	14.69	15.59	17.24	16.81
0.24975	23.70	18.40	19.97	23.71	23.36

A. Classical dynamics of the constant period oscillator

The relativistic classical dynamics of the CPO is governed by the Hamilton's equations of motion

$$\frac{dq}{dt} = \frac{p}{\sqrt{m^2 + p^2/c^2}}, \quad (27)$$

$$\frac{dp}{dt} = -\frac{dV(q)}{dq}, \quad (28)$$

where $V(q)$ represents the constant period potential of Sec. III. Even if we use the approximate potential V_1 or V_2 for the potential $V(q)$, it is not possible to obtain an analytic solution to Eqs. (27) and (28). The data reported in this section were thus obtained by numerically integrating Eqs. (27) and (28).

In Fig. 2 we show the time development of the position q , velocity v , and momentum $p = \gamma mv$ of the CPO for six different values of the initial energy for the case $m = T = c = 1$. The corresponding phase-space trajectories in the q - v plane and the q - p plane, respectively, are shown in Figs. 3(a) and 3(b). One can clearly see that the CPO behaves like the SHO of the same period at low energies ($E \ll mc^2$) and like a particle in a square-well potential of half-width $cT/4$ at ultrahigh energies ($E \gg c^2$).

At all energies, q , v , and p are all periodic with a given period T and can be expanded in Fourier series. Thus one can write $q(t)$ as

$$q(t) = \sum_{n \text{ odd}} a_n \cos \frac{2\pi nt}{T}, \quad (29)$$

where a_n 's in general depend on energy $a_n = a_n(E)$. At non-relativistic energies ($E \ll mc^2$), we have

$$a_n = \sqrt{\frac{ET^2}{2m\pi^2}} \delta_{n1}, \quad (30)$$

representing a sinusoidal wave, while in the ultrarelativistic limit ($E \gg mc^2$)

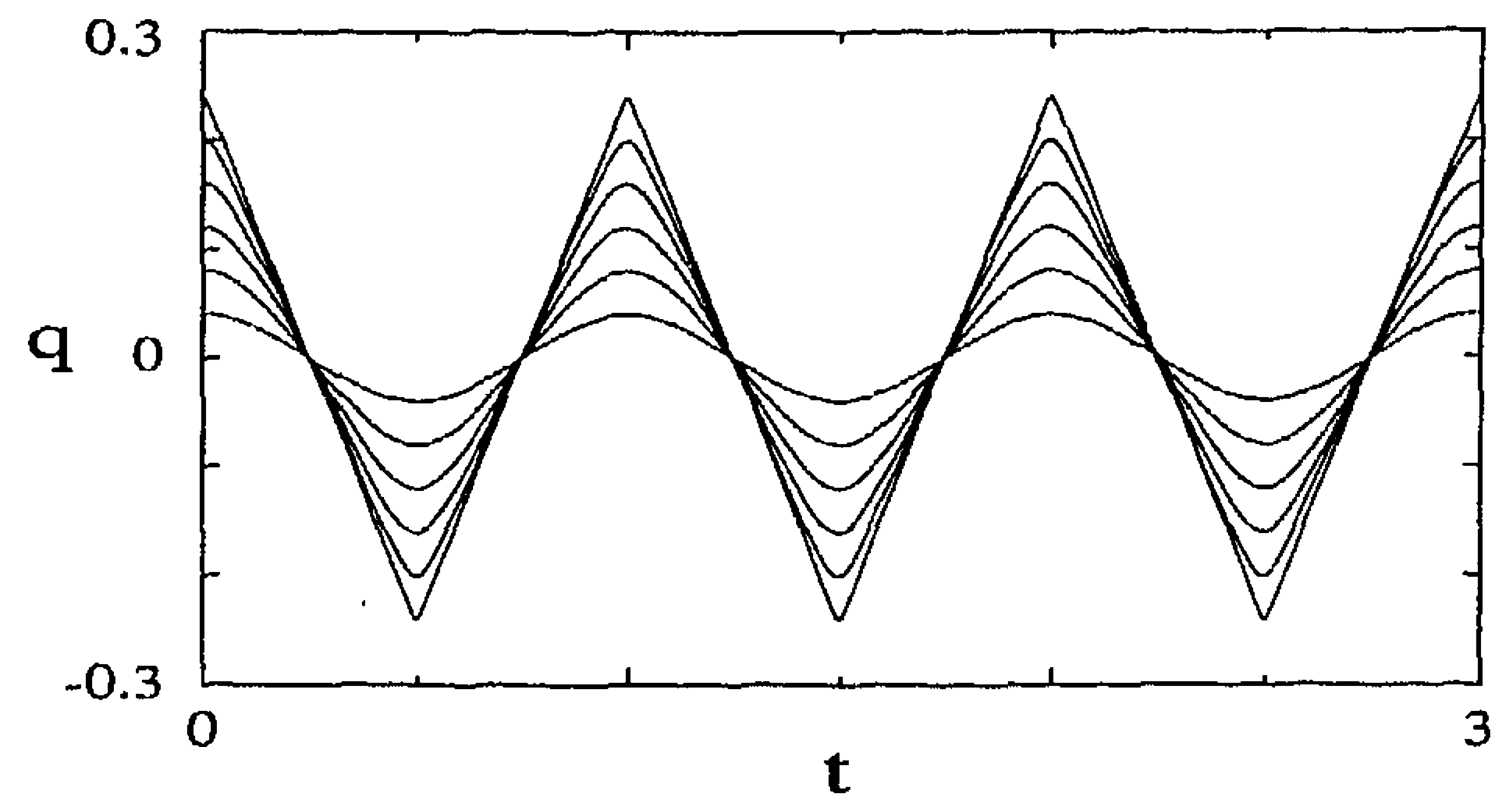
$$a_n = \frac{2cT}{\pi^2 n^2}, \quad n = 1, 3, 5, \dots, \quad (31)$$

representing a sawtooth wave.

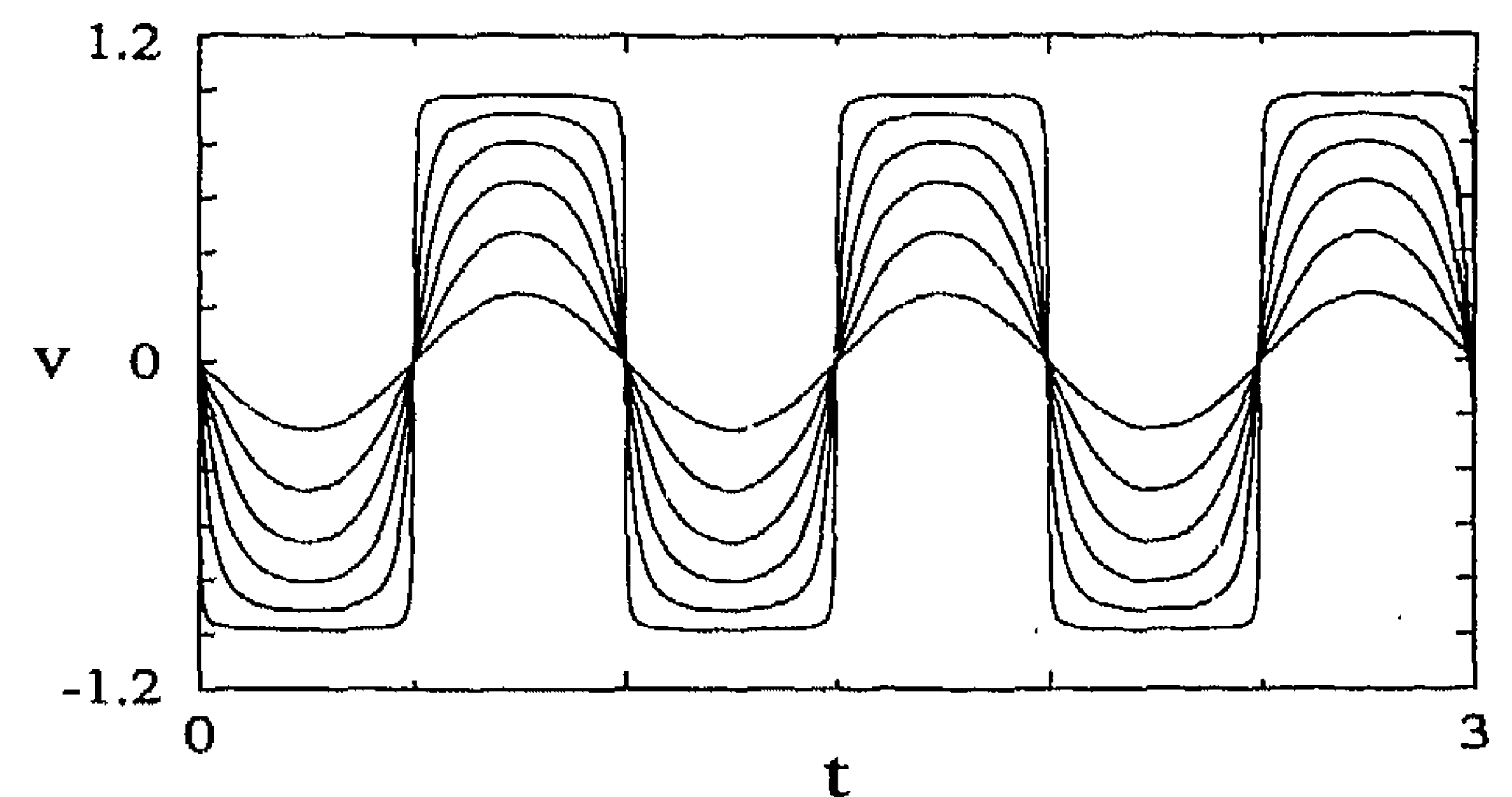
In Figs. 4(a) and 4(b) we plot the first six nonzero coefficients a_n obtained by numerical computation as a function of energy for the case $m = T = c = 1$. It can be seen that all the coefficients plotted tend to the values given by Eq. (31) as energy is increased to a high value. As energy is lowered, all coefficients decrease, but those with a larger n decrease faster. At low energies therefore high-order coefficients are relatively unimportant and a small number of low-order a_n 's are sufficient to describe the motion.

B. Quantum energy eigenvalues of the constant period oscillator

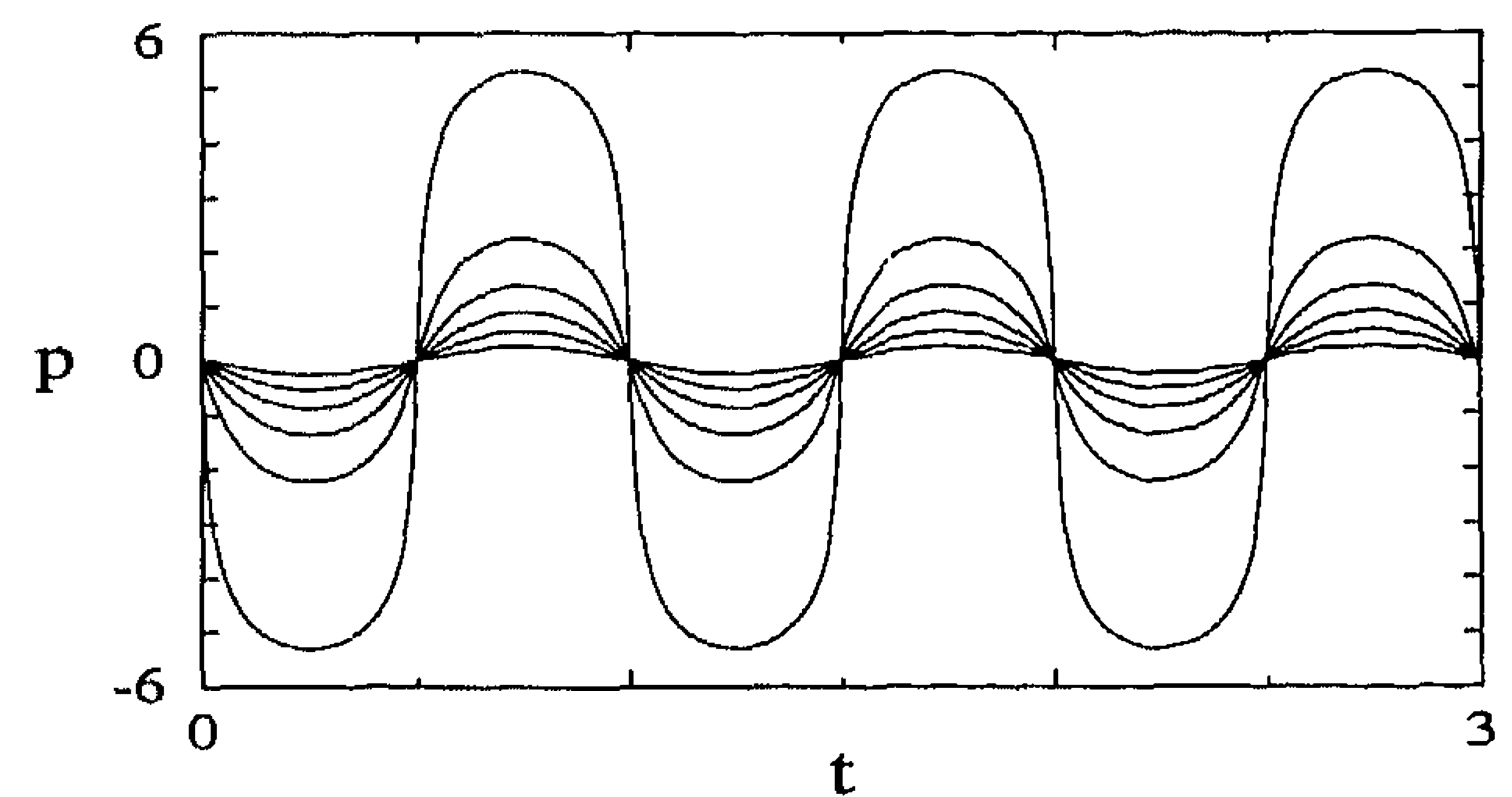
We now turn to a quantum-mechanical analysis of the CPO. In the nonrelativistic case, the constant period of the SHO manifests itself in quantum mechanics as equally



(a)



(b)



(c)

FIG. 2. Time development of the position q , velocity v , and momentum p of the constant period oscillator for six different initial conditions $(q_0, p_0) = (0.04, 0)$, $(0.08, 0)$, $(0.12, 0)$, $(0.16, 0)$, $(0.2, 0)$, and $(0.24, 0)$. $m = T = c = 1$.

spaced energy levels. This quantum-classical correspondence can best be seen by applying the Bohr-Sommerfeld quantization rule [12,13]

$$I = \frac{1}{2\pi} \oint p dq = \left(n + \frac{1}{2}\right) \frac{h}{2\pi} \quad (32)$$

to the SHO. Since Eq. (7) is valid for the SHO as long as we limit our consideration to nonrelativistic motion, we have from Eqs. (7) and (32)

$$E_n = \frac{2\pi}{T} I_n = \left(n + \frac{1}{2}\right) \frac{h}{T}. \quad (33)$$

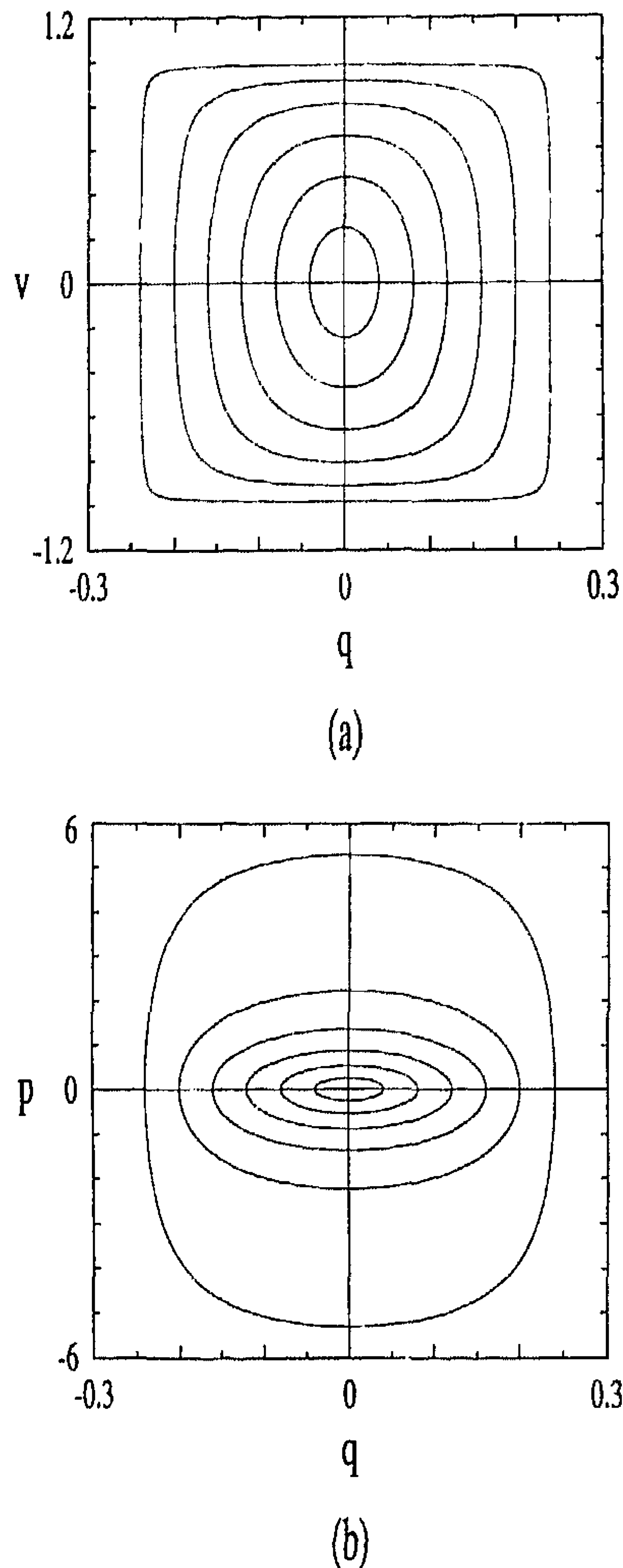


FIG. 3. (a) Phase-space trajectories in the q - v plane. Parameters $(q_0, p_0), m, T$ and c are the same as in Fig. 2. (b) Phase-space trajectories in the q - p plane. Parameters $(q_0, p_0), m, T$, and c are the same as in Fig. 2.

We see therefore that, for the case of the SHO, the Bohr-Sommerfeld quantization rule agrees exactly with the quantum-mechanical solution of the Schrödinger equation.

It is of interest to see if the above quantum-classical correspondence holds also for the CPO. In order to determine the energy eigenvalues of the CPO, we choose to solve the time-independent Klein-Gordon equation

$$-c^2\hbar^2\frac{\partial^2\psi}{\partial q^2} + m^2c^4\psi = [E + mc^2 - V(q)]^2\psi(q). \quad (34)$$

Let us first consider Eq. (34) in the ultrarelativistic limit ($E_n \gg mc^2$ for all n), in which case Eq. (34) can be written approximately as

$$-c^2\hbar^2\frac{\partial^2\psi}{\partial q^2} \cong E^2\psi. \quad (35)$$

Solving Eq. (35) for ψ and applying the boundary condition $\psi(q = \pm cT/4) = 0$, one can immediately obtain

$$E_n = (n+1)\frac{h}{T}. \quad (36)$$

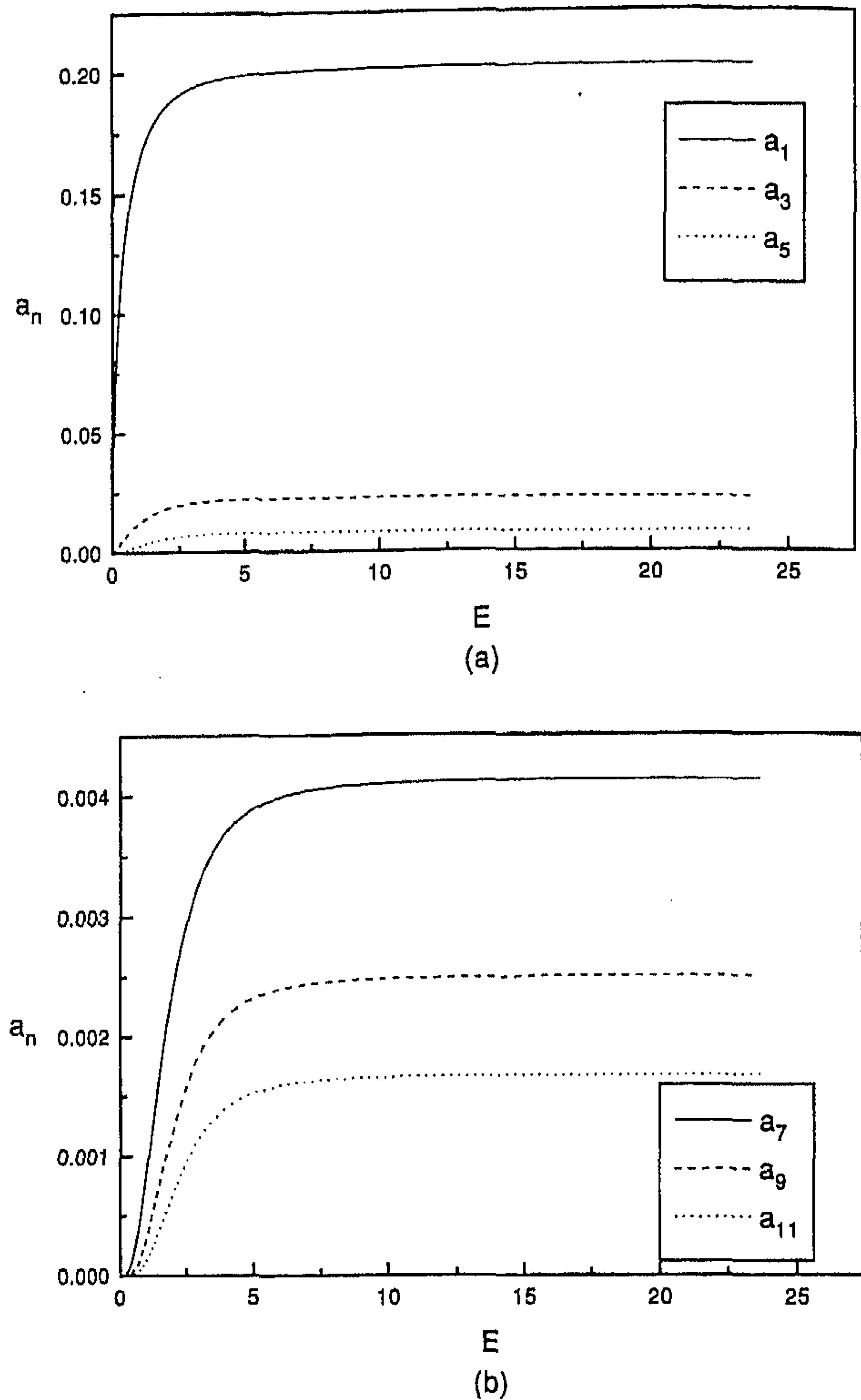


FIG. 4. (a) Fourier coefficients a_1, a_3 , and a_5 vs energy E . $m=T=c=1$. (b) Fourier coefficients a_7, a_9 , and a_{11} vs energy E . $m=T=c=1$.

Thus, for the case of an ultrarelativistic CPO ($\hbar/T \gg mc^2$), the Bohr-Sommerfeld quantization rule holds with the factor $\frac{1}{2}$ replaced by 1 and all energy levels of the CPO are equally spaced.

At arbitrary relativistic energies, the Klein-Gordon equation cannot be dealt with analytically in general. We thus integrated Eq. (34) numerically to determine energy eigenvalues. The eigenvalues thus obtained are presented in Table III for the case $m=T=1$ and $\hbar=0.1$ for three different values of c . At $c=10$ all energy eigenvalues listed are seen to be equally spaced. In this case the eigenvalues are well below $mc^2=100$ and thus the CPO behaves almost like the corresponding SHO. At both $c=0.6$ and $c=0.2$ deviations from equal spacing are clearly indicated. At $c=0.2$, in particular, the lowest-energy eigenvalue is already higher than mc^2 and thus relativistic effects cannot be neglected even when calculating the lowest-energy eigenvalue. We note, however, that, as we move to higher-energy levels, energy spacing tends to the value \hbar/T . This is in agreement with the above analysis leading to Eq. (36) for an ultrarelativistic CPO. We also note that the energy eigenvalue of the lowest state is in general different from $0.5(\hbar/T)$.

In order to better understand the numerical data presented in Table III, we need to look closely at the Bohr-Sommerfeld

TABLE III. Energy eigenvalues of the constant period oscillator. $m = T = 1$ and $h = 0.1$.

n	$c = 10$		$c = 0.6$		$c = 0.2$	
	$\frac{E_n}{h/T}$	$\frac{\Delta E_n}{h/T}$	$\frac{E_n}{h/T}$	$\frac{\Delta E_n}{h/T}$	$\frac{E_n}{h/T}$	$\frac{\Delta E_n}{h/T}$
0	0.500		0.496		0.752	
1	1.500	1.000	1.490	0.995	1.824	1.072
2	2.500	1.000	2.488	0.998	2.860	1.036
3	3.500	1.000	3.490	1.002	3.882	1.022
4	4.500	1.000	4.496	1.006	4.897	1.015
5	5.500	1.000	5.505	1.009	5.908	1.010
6	6.500	1.000	6.516	1.011	6.916	1.008
7	7.500	1.000	7.528	1.013	7.923	1.007
8	8.500	1.000	8.542	1.013	8.928	1.005
9	9.500	1.000	9.555	1.013	9.933	1.004

quantization rule. The Bohr-Sommerfeld quantization rule, as expressed in Eq. (32), can be understood to arise as a consequence of the fact that any adiabatically invariant quantity should be quantized and that the action variable I is an adiabatic invariant [14,15]. The integer n in Eq. (32) coincides with the number of de Broglie half waves contained between two classical turning points. The constant $\frac{1}{2}$ is related to penetration of the wave function into classically forbidden regions [15,16]. It should be noted, however, that this value of $\frac{1}{2}$ is obtained within the WKB approximation of nonrelativistic quantum mechanics under the condition that the potential can be sufficiently well approximated by a linear function in the immediate neighborhood of each turning point. One can thus suggest that a more accurate version of the Bohr-Sommerfeld quantization rule can be written as

$$I = \frac{1}{2\pi} \oint p dq = (n + 1 - \alpha) \frac{h}{2\pi}, \quad (37)$$

where the constant α takes on a different value depending on the degree of penetration of the wave function into classically forbidden regions. For a nonrelativistic simple harmonic oscillator, α is exactly $\frac{1}{2}$, whereas, for a nonrelativistic particle in an infinite potential well for which no penetration exists, it is exactly zero. For the case of a potential of com-

plex shape, such as the CPP being considered here, the constant α does not necessarily take on a single fixed value [16]. Rather, it is a function of energy or of the quantum number n , i.e., $\alpha = \alpha_n$. If we consider a nonrelativistic particle moving under the influence of the CPP, α should be a decreasing function of n because the potential becomes steeper and penetration weaker as energy is increased, leading eventually to a nonuniform spacing of energy levels. For a relativistic particle moving under the influence of the CPP, however, one may intuitively expect that associated energy levels are equally spaced. Our numerical data of Table III indicate, however, that they are not. Energy eigenvalues of the CPO are equally spaced only in the nonrelativistic and ultrarelativistic limits. Furthermore, the ground-state energy can be either higher or lower than $0.5(h/T)$. The Bohr-Sommerfeld quantization rule Eq. (32) is not in exact agreement with the solution of the Klein-Gordon equation for the case of the CPO.

ACKNOWLEDGMENTS

This research was supported in part by a KAIST Research Grant and by the Agency for Defense Development of Korea. The authors wish to thank Dr. Mike Keane of CWI, The Netherlands, for stimulating discussions.

- [1] H. Goldstein, *Classical Mechanics*, 2nd ed. (Addison-Wesley, Reading, MA, 1981), p. 324.
- [2] R. G. Newton, *Scattering Theory of Waves and Particles* (McGraw-Hill, New York, 1966), p. 140.
- [3] J. B. Keller, I. Kay, and J. Shmoys, *Phys. Rev.* **102**, 557 (1956).
- [4] M. R. Spiegel, *Theory and Problems of Laplace Transforms* (McGraw-Hill, New York, 1965), p. 113.
- [5] S. G. Kamath, *J. Math. Phys.* **33**, 934 (1992).
- [6] H. Funke and Y. Ratis, *Inverse Problems* **6**, L13 (1990).
- [7] J. H. Kim and H. W. Lee, *Phys. Rev. E* **51**, 1579 (1995).
- [8] J. H. Kim and H. W. Lee, *Phys. Rev. E* **52**, 473 (1995).

- [9] S. M. Soskin, *Phys. Rev. E* **50**, R44 (1994).
- [10] P. V. E. McClintock, S. M. Soskin, N. D. Stein, and N. G. Stocks, *Phys. Rev. E* **48**, 147 (1993).
- [11] B. V. Chirikov, *Phys. Rep.* **52**, 263 (1979).
- [12] L. D. Landau and E. M. Lifshitz, *Quantum Mechanics*, 3rd ed. (Pergamon, Oxford, 1977), p. 170.
- [13] M. Tabor, *Chaos and Integrability in Nonlinear Dynamics* (Wiley, New York, 1989), p. 233.
- [14] M. V. Berry, *Proc. R. Soc. London Ser. A* **429**, 61 (1990).
- [15] F. S. Crawford, *Am. J. Phys.* **58**, 337 (1990).
- [16] D. J. W. Geldart and D. Kiang, *Am. J. Phys.* **54**, 131 (1986).